Multiplicity fluctuations in limited segments of momentum space in statistical models

Michael Hauer
Helmholtz Research School, University of Frankfurt, Frankfurt, Germany
(Received 25 October 2007; published 31 March 2008)

Multiplicity fluctuations in limited segments of momentum space are calculated for a classical pion gas within the statistical model. Results for the grand canonical, canonical, and micro-canonical ensemble are obtained, compared, and discussed. We demonstrate that even in the large volume limit correlations between macroscopic subsystems due to energy and momentum conservation persist. Based on the microcanonical formulation we make qualitative predictions for the rapidity and transverse-momentum dependence of multiplicity fluctuations. The resulting effects are of similar magnitude as the predicted enhancement due to a phase transition from a quark-gluon plasma to a hadron gas phase or due to the critical point of strongly interacting matter and qualitatively agree with recently published preliminary multiplicity fluctuation data of the NA49 SPS experiment.

DOI: 10.1103/PhysRevC.77.034909 PACS number(s): 24.10.Pa, 24.60.Ky, 25.75.−q

I. INTRODUCTION

The statistical model has been, for a long time, successfully applied to fit experimental data on mean hadron multiplicities in heavy-ion collision experiments over a wide range of beam energies and system sizes. For recent reviews, see Refs. [1–4]. So naturally the question arises whether the statistical model is able to describe event-by-event fluctuations of these observables as well. And, indeed, a first comparison suggests that this might be possible for the sample of most central events. Global conservation laws, imposed on a statistical system, lead, even in the large volume limit, to suppressed fluctuations. The multiplicity distributions of charged hadrons recently reported [5] by the NA49 SPS experiment are systematically narrower than a Poissonian reference distribution. This could be interpreted [6] as effects due to energy and charge conservation in a relativistic hadronic gas.

Multiplicity fluctuations are usually quantified by the ratio of the variance of a multiplicity distribution to its mean value, the so-called scaled variance. In statistical models there is a qualitative difference in the properties of mean value and scaled variance. In the case of the mean multiplicity results obtained within the grand canonical ensemble (GCE), canonical ensemble (CE), and microcanonical ensemble (MCE) approach each other in the large volume limit. One refers here to the thermodynamic equivalence of these ensembles. It was recently found [7] that corresponding results for the scaled variance are different in different ensembles, and thus this observable is sensitive to conservation laws obeyed by a statistical system.

The growing interest in the experimental and theoretical study of fluctuations in strong interactions (see, e.g., Ref. [8]) is motivated by expectations of anomalies in the vicinity of the onset of deconfinement [9] and in the case when the expanding system goes through the transition line between a quark-gluon plasma and a hadron gas phase [10]. In particular, a critical point of strongly interacting matter may be accompanied by a characteristic power-law pattern in fluctuations [11]. A nonmonotonic dependence of event-by-event fluctuations on system size and/or center-of-mass energy in heavy-ion collisions would therefore give valuable insight into the phase diagram of strongly interacting matter. Provided the signal survives the subsequent evolution and hadronization of the system (see also Ref. [12]). Therefore, to asses the discriminating power of proposed measures (for a recent review, see Ref. [13]), one should first study properties of equilibrated sources [6,14–16] and quantify "baseline" (or thermal/statistical) fluctuations. Apart from being an important tool in an effort to study a possible critical behavior, the study of fluctuations within the statistical model constitutes also a further test of its validity.

In this article we make detailed predictions for the momentum-space dependence of multiplicity fluctuations. We show that energy and momentum conservation lead to a nontrivial dependence of the scaled variance on the location and magnitude of the observed fraction of momentum space. These predictions can be tested against existing and future data from the heavy-ion collision experiments at the CERN SPS and BNL RHIC facilities.

The article is organized as follows: In Sec. II we briefly introduce our model. In Sec. III we consider multiplicity distributions in a limited region of momentum space in GCE and CE. For the MCE we follow, in Sec. IV, the procedure of Ref. [17] and show how to calculate the width of the corresponding distributions in the large volume limit. We revisit the so-called acceptance scaling previously suggested as an approximate implementation of experimental acceptance in Sec. V. Technical details of the calculations are presented in the Appendix. Concluding remarks and a summary in Secs. VI and VII close the article.

II. THE MODEL

The ideal Boltzmann $\pi^+\pi^-\pi^0$ gas serves as the standard example throughout this article, whereas the main subject of investigation is the multiplicity distribution $P(N_\Omega)$ of particles with momenta inside a certain segment Ω of momentum space. Calculations are done for the three standard ensembles GCE, CE, and MCE. For the sake of argument we will assume that we want to measure only $P(N_\Omega^-)$, i.e., the probability

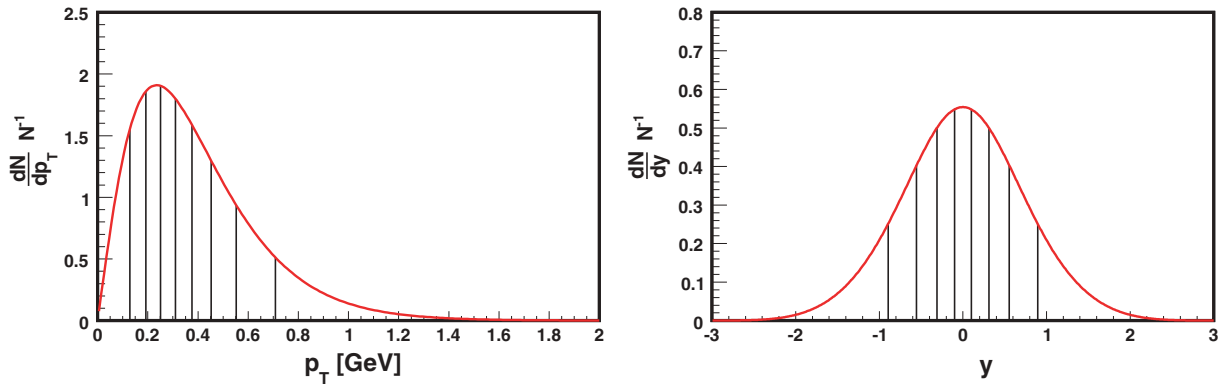

FIG. 1. (Color online) Differential particle spectra for a classical pion gas at $T = 160$ MeV. (Left) Transverse-momentum spectrum Eq. (B1). (Right) Rapidity spectrum Eq. (C1). Both curves are normalized to the total yield Eq. (6). The bins are constructed in a way that each bin contains 1/9 of the total yield.

distribution of negatively charged pions in a limited segment Ω of momentum space. Hence π^- with momenta inside Ω are observed, whereas π^- inside the complementary segment $\bar{\Omega}$ are not observed. π^+ and π^0 are never detected. In GCE and CE the presence of π^0 as a degree of freedom is of no relevance, whereas in MCE it constitutes a heat bath for the remaining system. For consistency we use the same system throughout this discussion.

To keep the model simple, we assume a static homogenous fireball. Our considerations therefore exclude collective motion, i.e., flow, and resulting momentum spectra are purely thermal. We also omit resonance decay contributions in this work. The spectra presented in Fig. 1 are normalized to the total π^- yield in GCE and CE. Thus they are the same in both ensembles. In MCE one expects in the large volume limit only small deviations from Boltzmann spectra. None of the forthcoming arguments are affected by this. In the following we will use the transverse-momentum and rapidity spectra presented in Fig. 1 to construct bins $\Omega_i = \Delta p_{Ti} = [p_{T_i}, p_{T_{i+1}}]$ (left) or $\Omega_i = \Delta y_i = [y_i, y_{i+1}]$ (right), as indicated by the drop lines.

In Sec. III we calculate the multiplicity distributions $P(N_\Omega)$ for arbitrary segments Ω for the ideal Boltzmann GCE and CE. To characterize the distribution one can calculate its (raw) moments $\langle N_\Omega^n \rangle$ from:

$$\left\langle N_\Omega^n \right\rangle = \sum_{N_\Omega=0}^{\infty} N_\Omega^n P\left(N_\Omega\right). \tag{1}$$

A convenient measure for the width of a distribution is the scaled variance:

$$\omega_\Omega \equiv \frac{\left\langle N_\Omega^2 \right\rangle - \langle N_\Omega \rangle^2}{\langle N_\Omega \rangle}. \tag{2}$$

To remove simple scaling effects, the bin sizes or segments are chosen such that each bin or segment contains the same fraction $q = \langle N_\Omega \rangle / \langle N_{4\pi} \rangle$ of the total yield [compare Eq. (2)]. Here $\langle N_\Omega \rangle$ denotes the average particle number in the momentum-space segment Ω, and $\langle N_{4\pi} \rangle$ denotes the average total (4π integrated) multiplicity. The effect of finite acceptance can approximately be taken into account by [7]:

$$\omega_q = 1 + q\left(\omega_{4\pi} - 1\right), \tag{3}$$

where $\omega_{4\pi}$ assumes the ideal situation when all particles are detected, whereas ω_q assumes that particles are detected with probability q regardless of their momentum. Hence Eq. (3) holds when particles are assumed to be uncorrelated in momentum space. In the limit $q \to 0$ one observes a random distribution with $\omega_q \to 1$, i.e., a Poissonian, whereas when $q \to 1$ one sees the real distribution with width $\omega_q \to \omega_{4\pi}$. In this work we take explicitly correlations due to globally conserved charge (CE) and energy-momentum (MCE) into account and compare the results to Eq. (3).

III. GRAND CANONICAL AND CANONICAL ENSEMBLE

A. Grand canonical ensemble

In the GCE, both heat and charge bath are assumed to be infinite. And thus charge, energy, and momentum are not conserved exactly. Temperature T and charge chemical potential μ regulate average energy and charge density in a system of volume V. Usually it is said that charge, energy, and momentum are conserved in the average sense and fluctuations about an equilibrium value are allowed. Apart form Bose and Fermi effects [18] particles are therefore uncorrelated in momentum space. However, this example serves as an illustration for the following CE and MCE calculations. We start by decomposing the Boltzmann single particle partition function $z^-(\phi_{N_\Omega})$ of π^- into two parts,

$$z^-\left(\phi_{N_\Omega}\right) = z_\Omega^-\left(\phi_{N_\Omega}\right) + z_{\bar{\Omega}}^- = \frac{gV}{(2\pi)^3}\int_\Omega d^3p e^{-\frac{\varepsilon+\mu}{T}} e^{i\phi_{N_\Omega}} + \frac{gV}{(2\pi)^3}\int_{\bar{\Omega}} d^3p e^{-\frac{\varepsilon+\mu}{T}}, \tag{4}$$

where the single-particle energy $\varepsilon = \sqrt{p^2 + m^2}$, and m and g are mass and degeneracy factor of π^-, respectively. Only for momentum states inside the momentum space region Ω do we introduce additionally a Wick-rotated fugacity $\exp(i\phi_{N_\Omega})$. For the positive and neutral pion (which we do not want to detect

in our example) we write:

$$z^+ = \frac{gV}{(2\pi)^3}\int d^3p e^{-\frac{\varepsilon-\mu}{T}} \quad \text{and} \quad z^0 = \frac{gV}{(2\pi)^3}\int d^3p e^{-\frac{\varepsilon}{T}}. \tag{5}$$

The value of the single-particle partition function, for instance, of the neutral pion, is given by:

$$z^0 = \langle N^0\rangle = \frac{gV}{2\pi^2}m^2TK_2\left(\frac{m}{T}\right). \tag{6}$$

For the sake of simplicity we assume equal masses for all pions. To obtain the GCE multiplicity distribution for N_Ω in a momentum-space segment Ω we use the Fourier integral over the generalized GCE partition function $\mathcal{Z}(\phi_{N_\Omega}) = \exp[z^-_\Omega(\phi_{N_\Omega}) + z^-_{\bar\Omega} + z^+ + z^0]$, normalized by the GCE partition function:

$$\begin{aligned} P_{\rm gce}(N_\Omega) &\equiv Z^{-1}_{\rm gce}\times\int_{-\pi}^{\pi}\frac{d\phi_{N_\Omega}}{2\pi}e^{-iN_\Omega\phi_{N_\Omega}}\mathcal{Z}\left(\phi_{N_\Omega}\right)\\ &= \frac{(z^-_\Omega)^{N_\Omega}}{N_\Omega!}\exp[-z^-_\Omega], \end{aligned} \tag{7}$$

where the system partition function is given by $Z_{\rm gce} \equiv \mathcal{Z}(\phi_{N_\Omega}=0)$ and $z^-_\Omega = z^-_\Omega(\phi_{N_\Omega}=0)$. Independent of the shape or size of Ω we find a Poissonian for the multiplicity distribution Eq. (7). Thus, using Eq. (2), one finds for the scaled variance $\omega^{\rm gce}_\Omega = 1$, because $\langle N_\Omega\rangle = z^-_\Omega$ and $\langle N^2_\Omega\rangle = \langle N_\Omega\rangle^2 + \langle N_\Omega\rangle$.

For Bose and Fermi statistics one does not expect a Poisson distribution and (in particular when the chemical potential is large) deviations from a Poissonian can be large. Thus one expects also deviations from Eq. (3) when considering only finite acceptance.

B. Canonical ensemble

In the CE the heat bath is still assumed to be infinite, while we remove the charge bath and drop the chemical potential. Thus, we introduce a further Wick-rotated fugacity $\mu/T \to i\phi_Q$ into the single-particle partition functions to account for global (however, not in the momentum-space segment Ω) conservation of electric charge Q. Particles in Ω are therefore correlated, due to the condition of fixed net charge, with a finite charge bath composed of π^+ and unobserved π^-. We again split the single-particle partition function for π^- into an observed, $z^-_\Omega(\phi_{N_\Omega},\phi_Q)$, and an unobserved part, $z^-_{\bar\Omega}(\phi_Q)$,

$$\begin{aligned} z^-\left(\phi_{N_\Omega},\phi_Q\right) &= z^-_\Omega\left(\phi_{N_\Omega},\phi_Q\right) + z^-_{\bar\Omega}(\phi_Q)\\ &= \frac{gV}{(2\pi)^3}\int_\Omega d^3p e^{-\frac{\varepsilon}{T}}e^{-i\phi_Q}e^{i\phi_{N_\Omega}}\\ &\quad + \frac{gV}{(2\pi)^3}\int_{\bar\Omega} d^3p e^{-\frac{\varepsilon}{T}}e^{-i\phi_Q}, \end{aligned} \tag{8}$$

whereas we do not want to measure π^+ and π^0 and thus:

$$z^+(\phi_Q) = \frac{gV}{(2\pi)^3}\int d^3p e^{-\frac{\varepsilon}{T}}e^{+i\phi_Q}$$

and

$$z^0 = \frac{gV}{(2\pi)^3}\int d^3p e^{-\frac{\varepsilon}{T}}. \tag{9}$$

The normalization of the CE multiplicity distribution is given by the CE system partition function $Z_{\rm ce}$, i.e., the number of all micro states with fixed charge Q, $Z^{\rm ce} = I_Q(2z)\exp(z^0)$, where I_Q is the modified Bessel function. The multiplicity distribution of N_Ω in a momentum-space segment Ω, whereas charge Q is globally conserved, can be obtained from Fourier integration of the generalized GCE partition function $\mathcal{Z}(\phi_{N_\Omega},\phi_Q) = \exp[z^-_\Omega(\phi_{N_\Omega},\phi_Q) + z^-_{\bar\Omega}(\phi_Q) + z^+(\phi_Q) + z^0]$, over both angles ϕ_Q and ϕ_{N_Ω}:

$$\begin{aligned} &P_{\rm ce}(N_\Omega)\\ &\equiv Z^{-1}_{\rm ce}\times\int_{-\pi}^{\pi}\frac{d\phi_{N_\Omega}}{2\pi}\int_{-\pi}^{\pi}\frac{d\phi_Q}{2\pi}e^{-iN_\Omega\phi_{N_\Omega}}e^{-iQ\phi_Q}\mathcal{Z}\left(\phi_{N_\Omega},\phi_Q\right) \end{aligned} \tag{10}$$

$$= I^{-1}_Q(2z)\times\frac{(z^-_\Omega)^{N_\Omega}}{N_\Omega!}\sum_{a=0}^{\infty}\frac{(z^-_{\bar\Omega})^a}{a!}\frac{z^{Q+N_\Omega+a}}{(Q+N_\Omega+a)!}, \tag{11}$$

where in CE $z^-_\Omega = z^-_\Omega(\phi_{N_\Omega}=\phi_Q=0)$, $z^-_{\bar\Omega} = z^-_{\bar\Omega}(\phi_Q=0)$, and $z = z^+(\phi_Q=0) = z^0$. For the respective first two moments one finds from Eq. (1):

$$\langle N_\Omega\rangle = z^-_\Omega\frac{I_{Q+1}(2z)}{I_Q(2z)}$$

and

$$\left\langle N^2_\Omega\right\rangle = (z^-_\Omega)^2\frac{I_{Q+2}(2z)}{I_Q(2z)} + z^-_\Omega\frac{I_{Q+1}(2z)}{I_Q(2z)}. \tag{12}$$

Thus, we obtain the well-known canonical suppression of yields [19–22] and fluctuations [7,23]. The result, however, is completely independent of the position of the segment Ω. And therefore the scaled variance, Eq. (2), takes the form:

$$\omega^{\rm ce}_\Omega = 1 + z^-_\Omega\left[\frac{I_{Q+2}(2z)}{I_{Q+1}(2z)} - \frac{I_{Q+1}(2z)}{I_Q(2z)}\right]$$

and

$$\omega^{\rm ce}_{4\pi} = 1 + z\left[\frac{I_{Q+2}(2z)}{I_{Q+1}(2z)} - \frac{I_{Q+1}(2z)}{I_Q(2z)}\right], \tag{13}$$

where ω_Ω is the width of $P_{\rm ce}(N_\Omega)$, i.e., the multiplicity distribution of π^- with momenta inside Ω, whereas $\omega_{4\pi}$ is the width of the corresponding distribution when Ω is extended to the full momentum space. It can immediately be seen that this formula is consistent with acceptance scaling, Eq. (3), $\omega_\Omega = 1 + q(\omega_{4\pi} - 1)$, if $q \equiv z^-_\Omega/z$. Generally we find $\omega^{\rm ce}_{4\pi} < \omega^{\rm ce}_\Omega < \omega^{\rm gce} = 1$. In the limit of $z^-_\Omega/z \to 0$ we approach the Poisson limit of a "random" distribution with $\omega = 1$, i.e., the observed part of the system is embedded into a much larger charge bath and the GCE is a valid description.

IV. MICROCANONICAL ENSEMBLE

For the MCE an analytical solution seems to be out of reach presently, so we use instead the asymptotic solution, applicable to large systems, derived in Ref. [17]. To avoid unnecessary repetition of calculations, we give only a general outline here and refer the reader for a detailed discussion to Ref. [17]. It should be mentioned that this method be would be also applicable to systems of finite spatial extention, provided

the average particle number in a given momentum space bin exceeds roughly $\langle N_\Omega \rangle \gtrsim 5$. In this work we confine ourselves to large systems and try to asses the general trends.

The basic idea is to define the MCE multiplicity distribution in terms of a joint GCE distribution of multiplicity, charge, energy, momentum, etc. The MCE multiplicity distribution is then given by the (normalized) conditional probability in the GCE to find a number N_Ω of particles in a segment Ω of momentum space, whereas electric charge Q, energy E, and three-momentum $\vec{P}$ are fixed. Therefore we will keep temperature and chemical potentials as parameters to describe our system. Effective temperature and effective chemical potential, i.e., Lagrange multipliers, can be determined by demanding that the GCE partition function is maximized for a certain equilibrium state $(Q, E, \vec{P})$. This requirement is entirely consistent [17] with the usual textbook definitions of T and μ in MCE and CE through differentiation of entropy and Helmholtz free energy with respect to conserved quantities. In principle we would have to treat all conservation laws on equal footing [24] and thus introduce Lagrange multipliers for momentum conservation as well. However, here we are only interested in a static source, thus $\vec{P} = \vec{0}$, and the relevant parameters are equal to zero.

In the large volume limit energy, charge, and particle density in the MCE will correspond to GCE values. This is required by the thermodynamic equivalence of ensembles for mean quantities. MCE and CE partition functions are generally obtained from their GCE counterpart by multiplication with δ functions, which pick out a set of micro states consistent with a particular conservation law. Here it will be of considerable advantage to use Fourier representations of δ functions, similar to the treatment in Sec. III. This method could be considered to be a Fourier spectral analysis of the generalized GCE partition function [17].

The normalized conditional probability distribution of multiplicity N_Ω can be defined by the ratio of the values of two partition functions:

$$P_{\mathrm{mce}}(N_\Omega) \equiv \frac{\text{number of all states with } N_\Omega,\ Q,\ E,\ \text{and } \vec{P} = \vec{0}}{\text{number of all states with } Q,\ E,\ \text{and } \vec{P} = \vec{0}}. \tag{14}$$

The real MCE partition function and our modified version are connected as $Z(V, N_\Omega, Q, E, \vec{P}) \equiv \mathcal{Z}^{N_\Omega, Q, E, \vec{P}}(V, T, \mu) e^{+E/T} e^{-Q\mu/T}$. In either case the normalization in Eq. (14) is given by the partition functions with fixed values of $Q, E, \vec{P}$, but arbitrary particle number N_Ω, hence $Z(V, Q, E, \vec{P}) \equiv \sum_{N_\Omega=0}^{\infty} Z(V, N_\Omega, Q, E, \vec{P})$ or $\mathcal{Z}^{Q, E, \vec{P}}(V, T, \mu) \equiv \sum_{N_\Omega=0}^{\infty} \mathcal{Z}^{N_\Omega, Q, E, \vec{P}}(V, T, \mu)$. However, when taking the ratio (14) auxiliary parameters chemical potential and temperature drop out:

$$P_{\mathrm{mce}}(N_\Omega) \equiv \frac{Z(V, N_\Omega, Q, E, \vec{P})}{Z(V, Q, E, \vec{P})} = \frac{\mathcal{Z}^{N_\Omega, Q, E, \vec{P}}(V, T, \mu)}{\mathcal{Z}^{Q, E, \vec{P}}(V, T, \mu)}. \tag{15}$$

The main difference between the two versions of partition functions is that for $Z(V, N_\Omega, Q, E, \vec{P})$ one is confronted with a heavily oscillating (or even irregular) integrant, whereas for $\mathcal{Z}^{N_\Omega, Q, E, \vec{P}}(V, T, \mu)$ the integrant becomes (T, μ correctly chosen) very smooth. Thus, introduction of T and μ allows to derive (and use) the asymptotic solution of Ref. [17].

We have a total number of six conserved "charges" and hence we need to solve the six-dimensional Fourier integral for the numerator in Eq. (15)[1]:

$$\begin{aligned}
&\mathcal{Z}^{N_\Omega, Q, E, \vec{P}} \\
&= \int_{-\pi}^{\pi} \frac{d\phi_{N_\Omega}}{2\pi} \int_{-\pi}^{\pi} \frac{d\phi_Q}{2\pi} \int_{-\infty}^{\infty} \frac{d\phi_E}{2\pi} \int_{-\infty}^{\infty} \frac{d\phi_{P_x}}{2\pi} \int_{-\infty}^{\infty} \frac{d\phi_{P_y}}{2\pi} \\
&\quad \times \int_{-\infty}^{\infty} \frac{d\phi_{P_z}}{2\pi} e^{-i N_\Omega \phi_{N_\Omega}} e^{-i Q \phi_Q} e^{-i E \phi_E} e^{-i P_x \phi_{P_x}} e^{-i P_y \phi_{P_y}} \\
&\quad \times e^{-i P_z \phi_{P_z}} \exp\left[V \sum_k \psi_k \left(\phi_{N_\Omega} \phi_Q, \phi_E, \phi_{P_x}, \phi_{P_y}, \phi_{P_z} \right) \right].
\end{aligned} \tag{16}$$

The summation in Eq. (16) should be taken over the single-particle partitions $V\psi_k = z_k$ of all considered particle species k. The Wick-rotated fugacities ϕ_Q, etc., are related to the individual conservation laws. The distinction between the Kronecker δ function (limits of integration $[-\pi, \pi]$) for discrete quantities and the Dirac δ function (limits of integration $[-\infty, \infty]$) for continuous quantities is important here; however, for deriving an asymptotic solution it will not be. To simplify Eq. (16) we change to shorthand notation for $\phi_j = (\phi_{N_\Omega} \phi_Q, \phi_E, \vec{\phi}_P)$ and the conserved "charge" vector $Q^j = (N_\Omega, Q, E, \vec{P})$. We again split the single-particle partition functions in two parts. The first part counts the number of momentum states observable to our detector, whereas the second part counts momentum states invisible to our detector:

$$\begin{aligned}
\psi_k(\phi_j) &= \frac{g_k}{(2\pi)^3} \int_\Omega d^3p\, e^{-\frac{\varepsilon_k - q_k \mu}{T}} e^{i q^j_{k,\Omega} \phi_j} \\
&\quad + \frac{g_k}{(2\pi)^3} \int_{\bar{\Omega}} d^3p\, e^{-\frac{\varepsilon_k - q_k \mu}{T}} e^{i q^j_{k,\bar{\Omega}} \phi_j}.
\end{aligned} \tag{17}$$

For the "charge" vector of all measured particle species k we write $q^j_{k,\Omega} = (1, q_k, \varepsilon_k, \vec{p}_k)$ for momenta inside Ω and $q^j_{k,\bar{\Omega}} = (0, q_k, \varepsilon_k, \vec{p}_k)$ for momenta outside of Ω. For all unobserved particle species we write $q^j_{k,\Omega} = q^j_{k,\bar{\Omega}} = (0, q_k, \varepsilon_k, \vec{p}_k)$. Here q_k is the electrical charge of particle species k, and ε_k and $\vec{p}_k$ are its energy and momentum vector. In Ref. [17], where only multiplicity distributions in the full momentum space were considered, the general "charge" vector took the form $q^j_{k,4\pi} = (n_k, q_k, \varepsilon_k, \vec{p}_k)$, where n_k is the multiplicity of this particle. For stable particles $n_k = 1$ in case they are observed, and $n_k = 0$ if they are not measured, whereas for unstable particles n_k could also denote the number of measurable decay products.

The real part of the integrant of the integral Eq. (16) has a sharp maximum around $\vec{\phi} = \vec{0}$, with both the peak height as

[1] We drop in the following the argument (V, T, μ) to simplify the notation.

well as the second derivative being proportional to the GCE partition function $Z_{\rm gce}$. (The imaginary part is antisymmetric.) For large system volume the main contribution to the integral (16) comes therefore from a small region around the origin [15]. Thus we proceed by Taylor expansion of the integrant of Eq. (16) around $\phi_j = \vec{0}$. In this context $\Psi(\phi_j) = \sum_k \psi_k(\phi_j)$ would be called the cumulant generating function (CGF). Cumulants (expansion terms) are defined by differentiation of the CGF at the origin:

$$\kappa_n^{j_1,j_2,\ldots,j_n} \equiv (-i)^n \left.\frac{\partial^n \Psi(\phi_j)}{\partial\phi_{j_1}\partial\phi_{j_2}\ldots\partial\phi_{j_n}}\right|_{\phi_j=\vec{0}}. \tag{18}$$

Generally are cumulants tensors of rank n and dimension defined by the number of conserved quantities. Here κ_1 is a six-component vector, while κ_2 is a 6×6 matrix, etc.

The parts of the integrant related to discrete quantities, i.e., N_Ω and Q, are now not 2π periodic anymore [whereas in Eq. (16) they are] but superpositions of oscillating and decaying parts. Thus we extent the limits of integration to $\pm\infty$, what introduces a negligible error. Equation (16) therefore simplifies to:

$$\mathcal{Z}^{Q^j} \simeq \left(\prod_{j=1}^{6}\int_{-\infty}^{\infty}\frac{d\phi_j}{(2\pi)}\right)\exp\left(-i\,Q^j\phi_j + V\sum_{n=0}^{\infty}\frac{i^n}{n!}\,\kappa_n^{j_1,j_2,\ldots,j_n}\phi_{j_1}\phi_{j_2}\ldots\phi_{j_n}\right). \tag{19}$$

Summation over repeated indices is implied. Existence and finiteness of the first three cumulants provided, any such integral can be shown to converge to a multivariate normal distribution in the large volume limit:

$$\mathcal{Z}^{Q^j} \simeq Z_{\rm gce}\frac{\exp\left(-\frac{\xi^j\,\xi_j}{2}\right)}{(2\pi V)^{6/2}\det|\sigma|}, \tag{20}$$

where $Z_{\rm gce}\equiv\exp[V\kappa_0]$ is the GCE partition function, κ_0 is the cumulant of 0th order, $\xi^j = (Q^k - V\kappa_1^k)(\sigma^{-1})_k{}^j V^{-1/2}$ is (in the large volume limit) a measure for the distance of a particular macro state Q^k to the peak $V\kappa_1^k$ of the joint distribution, and σ is the square root of the second rank tensor κ_2. The expansion Eq. (19) converges to the approximation Eq. (20) for sufficiently large volume, as long as higher-order expansion terms κ_n, $(n\geqslant 3)$ remain finite. This is the case for the model considered here. For a detailed derivation and calculation of finite volume corrections, see Ref. [17] for details.

The normalization in Eq. (15) can essentially be found in two ways. The first way would be to integrate the distribution (20) over all possible values of multiplicity N_Ω, while all other variables are set to their peak values, e.g., $Q = V\kappa_1^Q$, $E = V\kappa_1^E$, $\vec{P} = \vec{0}$. The second and more practical way is to use an approximation similar to Eq. (20) to describe the macro state $Q^j = (Q, E, \vec{P})$. The normalization in Eq. (15), $\mathcal{Z}^{E,Q,\vec{P}}$, is then given by the five-dimensional integral, similar to Eq. (16), without the integration over ϕ_{N_Ω}. The one-dimensional slice along N_Ω, i.e., the conditional distribution of particle number N_Ω, while charge, energy, and momentum are fixed to Q, E, $\vec{P} = \vec{0}$, can then be shown [17] to converge to a Gaussian in the large volume limit:

$$P_{\rm mce}(N_\Omega) \simeq \frac{1}{\left(2\pi\,\omega_\Omega^{\rm mce}\langle N_\Omega\rangle\right)^{1/2}}\exp\left[-\frac{(N_\Omega - \langle N_\Omega\rangle)^2}{2\omega_\Omega^{\rm mce}\langle N_\Omega\rangle}\right]. \tag{21}$$

The scaled variance $\omega_\Omega^{\rm mce}$ is given by the ratio of the two determinants of the two relevant second-rank cumulants, κ_2 and $\tilde{\kappa}_2$, of the two partition functions $\mathcal{Z}^{N_\Omega,E,Q,\vec{P}}$ and $\mathcal{Z}^{E,Q,\vec{P}}$, hence[2]:

$$\omega_\Omega^{\rm mce} = \frac{\det|\kappa_2|}{\kappa_1^{N_\Omega}\,\det|\tilde{\kappa}_2|}. \tag{22}$$

The asymptotic ($V\to\infty$) scaled variance can therefore be written in the form of Eq. (28) in Ref. [17]. For an explicity derivation of Eqs. (21) and (22) the reader is referred to Sec. III and Appendix D of Ref. [17]. Considering only the asymptotic solution we need to investigate only the first two cumulants ($n = 1, 2$) in detail. We will first discuss the structure of κ_1 and κ_2 and then deduce a few properties of Eq. (22).

The first-order cumulant κ_1 of $\mathcal{Z}^{N_\Omega,Q,E,\vec{P}}$ gives GCE expectation values for particle density $\kappa_1^{N_\Omega}$, charge density κ_1^Q, energy density κ_1^E, and expectation values of momentum $\kappa_1^{p_x}$, etc. Because we are only interested in a static source we find due to the antisymmetric momentum integral (see Appendix A) $\kappa_1^{p_x} = \kappa_1^{p_y} = \kappa_1^{p_z} = 0$. The general form of the first cumulant κ_1 is then:

$$\kappa_1 = \left(\kappa_1^{N_\Omega}, \kappa_1^Q, \kappa_1^E, 0, 0, 0\right). \tag{23}$$

The second cumulant κ_2 of $\mathcal{Z}^{N_\Omega,Q,E,\vec{P}}$ contains information about correlations due to different conserved quantities. A detailed discussion of correlation terms only involving Abelian charges and/or energy, e.g., $\kappa_2^{Q,Q}$, $\kappa_2^{Q,E}$, and $\kappa_2^{E,E}$, can be found in Ref. [17]. Again, due to the antisymmetric nature of the momentum integral, all cumulant entries involving an odd order in one of the momenta, e.g., κ_2^{E,p_x}, $\kappa_2^{p_x,p_y}$, or κ_2^{Q,p_x}, are equal to zero. The general second-order cumulant κ_2 thus reads:

$$\kappa_2 = \begin{Bmatrix} \kappa_2^{N_\Omega,N_\Omega} & \kappa_2^{N_\Omega,Q} & \kappa_2^{N_\Omega,E} & \kappa_2^{N_\Omega,p_x} & \kappa_2^{N_\Omega,p_y} & \kappa_2^{N_\Omega,p_z} \\ \kappa_2^{Q,N_\Omega} & \kappa_2^{Q,Q} & \kappa_2^{Q,E} & 0 & 0 & 0 \\ \kappa_2^{E,N_\Omega} & \kappa_2^{E,Q} & \kappa_2^{E,E} & 0 & 0 & 0 \\ \kappa_2^{p_x,N_\Omega} & 0 & 0 & \kappa_2^{p_x,p_x} & 0 & 0 \\ \kappa_2^{p_y,N_\Omega} & 0 & 0 & 0 & \kappa_2^{p_y,p_y} & 0 \\ \kappa_2^{p_z,N_\Omega} & 0 & 0 & 0 & 0 & \kappa_2^{p_z,p_z}. \end{Bmatrix} \tag{24}$$

Please note that by construction, Eq. (18), the matrix (27) is symmetric, hence $\kappa_2^{N_\Omega,Q} = \kappa_2^{Q,N_\Omega}$, etc.

The second matrix $\tilde{\kappa}_2$, now related to the partition function $\mathcal{Z}^{Q,E,\vec{P}}$, is obtained from κ_2, Eq. (27), by crossing out the first row and first column. In the following we are going to make

[2]Please note, that to simplify formulas, the notation is slightly different from Ref. [17].

use of the fact that one can express the determinant of a matrix A by:

$$\det|A| = \sum_{j=1}^{n} (-1)^{j+k} A_{j,k} M_{j,k}, \tag{25}$$

where $A_{j,k}$ is the matrix element j,k of a general nonsingular $n \times n$ matrix A and $M_{j,k}$ is its complementary minor. A simple consequence of Eq. (25) is:

$$\begin{aligned}\det|\tilde{\kappa}_2| &= \kappa_2^{p_x,p_x}\kappa_2^{p_y,p_y}\kappa_2^{p_z,p_z}\left[\kappa_2^{E,E}\kappa_2^{Q,Q} - \left(\kappa_2^{E,Q}\right)^2\right] \\ &= \left(\kappa_2^{p_x,p_x}\right)^3 \det|\hat{\kappa}_2|,\end{aligned} \tag{26}$$

where $\kappa_2^{p_x,p_x} = \kappa_2^{p_y,p_y} = \kappa_2^{p_z,p_z}$, due to spherical symmetry in momentum space, and $\hat{\kappa}_2$ is just a 2×2 matrix involving only terms containing E and Q. In case correlations between particle number and conserved momenta are vanishing, i.e., $\kappa_2^{N_{4\pi},p_x} = 0$ or $\kappa_2^{N_\Omega,p_x} = 0$, then, similarly to Eq. (26), the determinant of κ_2 factorizes into a product of correlation terms $(\kappa_2^{p_x,p_x})^3$ and the determinant of a 3×3 submatrix involving only terms containing E, Q, and N. Hence in taking the ratio Eq. (22) one notes that in this case momentum conservation will not affect multiplicity fluctuations in the large volume limit [17]. In this work, however, we do not necessarily find $\kappa_2^{N_\Omega,p_x} = 0$, as we integrate over only a limited segment Ω of momentum space, and taking momentum conservation into account may affect the result.

Finally, it should be stressed that this procedure can be easily generalized to account for Bose or Fermi statistics. Also phenomenological phase-space suppression (enhancement) factors γ_q [25] or γ_s [26] could be straightforwardly included. However, without proper implementation of the effect of additional correlations due to resonance decay and collective motion, i.e., flow, it seems of little value to do too strict calculations for experimentally measurable distributions. We thus return to the pion gas example from Sec. III and restrict the discussion to simple momentum space cuts in rapidity, transverse momentum, and azimuthal angle; see also the Appendix for details.

V. RESULTS

A. Multiplicity fluctuations in the full momentum space

Let us first recall basic properties of multiplicity fluctuations of negative particles in the full momentum space (4π fluctuations) in the three standard ensembles of the Boltzmann pion gas considered here.

Multiplicity fluctuations in the CE are suppressed due to exact charge conservation. For a neutral ($Q = 0$) system one finds in the large volume limit $\omega_{4\pi}^{\mathrm{ce}} = 0.5$ [7]. Further suppression of fluctuations arise from additionally enforcing exact energy conservation in the MCE. Here one finds $\omega_{4\pi}^{\mathrm{mce}} \approx 0.25$ for a Boltzmann pion gas at $T \approx 160$ MeV. In the GCE, because no conservation laws are enforced, we always find a Poisson distribution with width $\omega_{4\pi}^{\mathrm{gce}} = 1$.

Because charge conservation in CE links the distributions of negatively charged particles to the one of their positive counterparts, i.e., $P(N_-) = P(N_+ - Q)$, the relative width of $P(N_-)$ increases (decreases) as we move the electric charge density to positive (negative) values [27]. This can be easily be seen from Eq. (27) by crossing out all rows and columns containing energy and momentum. The second-order CE cumulant κ_2^{ce} is:

$$\kappa_2^{\mathrm{ce}} = \begin{pmatrix} \kappa_2^{N_{4\pi},N_{4\pi}} & \kappa_2^{N_{4\pi},Q} \\ \kappa_2^{Q,N_{4\pi}} & \kappa_2^{Q,Q} \end{pmatrix}. \tag{27}$$

One can then calculating the asymptotic CE scaled variance of negatively charged particles, $\omega_{4\pi}^{\mathrm{ce}}$, from Eq. (22),

$$\omega_{4\pi}^{\mathrm{ce}} = \frac{\kappa_2^{N_{4\pi},N_{4\pi}}\kappa_2^{Q,Q} - \left(\kappa_2^{N_{4\pi},Q}\right)^2}{\kappa_1^{N_{4\pi}}\kappa_2^{Q,Q}}. \tag{28}$$

For the ideal Boltzmann pion gas one finds for the expectation value of particle number density of negatively charged pions:

$$\begin{aligned}\kappa_1^{N_{4\pi}} &= \left(-i\,\frac{\partial}{\partial\phi_{N_{4\pi}}}\right)\Psi(\phi_j)\Big|_{\phi_j=\vec{0}} \\ &= \frac{g}{2\pi^2}m^2 T K_2\left(\frac{m}{T}\right)e^{-\frac{\mu}{T}} = \psi_- = \psi_0 e^{-\frac{\mu}{T}},\end{aligned} \tag{29}$$

where $\Psi(\phi_j) = \psi_-(\phi_j) + \psi_+(\phi_j) + \psi_0(\phi_j)$ is the CGF of ideal Boltzmann pion gas, and $\psi_k(\phi_j)$ are the single-particle partition functions given by Eq. (17) of π^-, π^+, and π^0 respectively. Further one finds from Eq. (18) in Boltzmann approximation:

$$\kappa_2^{N_{4\pi},N_{4\pi}} = \kappa_2^{N_{4\pi},Q} = \kappa_1^{N_{4\pi}}. \tag{30}$$

Fluctuations of electric charge in the GCE pion gas are given by:

$$\begin{aligned}\kappa_2^{Q,Q} &= \left(-i\,\frac{\partial}{\partial\phi_Q}\right)^2\Psi(\phi_j)\Big|_{\phi_j=\vec{0}} = \psi_0 e^{+\frac{\mu}{T}} + \psi_0 e^{-\frac{\mu}{T}} \\ &= 2\psi_0\cosh\left(\frac{\mu}{T}\right).\end{aligned} \tag{31}$$

Substitution of above relations into Eq. (28) leads to the result known from Ref. [27]:

$$\omega_{4\pi}^{\mathrm{ce}} = \frac{\exp\left(\frac{\mu}{T}\right)}{2\cosh\left(\frac{\mu}{T}\right)}. \tag{32}$$

The same effect is present in the MCE; however, the calculation is slightly longer.

Results for 4π multiplicity fluctuations of negatively charged particles in a Boltzmann pion gas at $T = 160$ MeV and different charge densities are summarized in Table I.

TABLE I. Multiplicity fluctuation of π^- in a classical pion gas in the large volume limit in the three standard ensembles at $T = 160$ MeV for different charge densities. The index "4π" denotes fluctuations in the full momentum space, whereas the index "$q = 1/9$" assumes acceptance scaling, Eq. (3). The ratio n_-/n_{tot} equals to 0.33 for $\mu = 0$, 0.48 for $\mu = -m/2$, and 0.20 for $\mu = +m/2$.

	$\omega_{4\pi}^{\mathrm{gce}}$	$\omega_{4\pi}^{\mathrm{ce}}$	$\omega_{4\pi}^{\mathrm{mce}}$	$\omega_{q=1/9}^{\mathrm{gce}}$	$\omega_{q=1/9}^{\mathrm{ce}}$	$\omega_{q=1/9}^{\mathrm{mce}}$
$\mu = 0$	1	0.5	0.235	1	0.944	0.915
$\mu = -\frac{m}{2}$	1	0.294	0.147	1	0.922	0.905
$\mu = +\frac{m}{2}$	1	0.706	0.353	1	0.967	0.928

Additionally estimates, based on our previously employed "uncorrelated particle" approach, Eq. (3), for multiplicity fluctuations with limited acceptance are given. Despite the fact that $\omega_{4\pi}$ is very different in GCE, CE, or MCE and also rather sensitive to the charge density, the estimates for limited acceptance ($q = 1/9$) based on Eq. (3) vary only by a few percentages. To decisively distinguish predictions for different ensembles a large value of q would be needed.

B. Multiplicity fluctuations in limited segments of momentum space

In Sec. III we have seen that in the Boltzmann CE multiplicity fluctuations observed in a limited segment of phase space are insensitive to the position of this segment. The dependence on the size of the segment can thus be taken into account by use of acceptance scaling Eq. (3). To balance charge a particle can be produced or annihilated anywhere in momentum space. And due to a infinitely large heat and momentum bath in the CE no momentum state is essentially preferred.

In the MCE this dependence is qualitatively different. When using the MCE formulation particles are correlated due to the constraints of exactly conserved energy and momentum, even in the large volume limit. Fluctuations in a macroscopic subsystem are strongly affected by correlations with the remainder of the system.

In Fig. 2 we show the scaled variance of multiplicity fluctuations for negatively charges particles in finite bins in transverse momentum (left) and rapidity (right). The bins are constructed such that each bin contains on average the same fraction q of the total average yield. The width of each bin is indicated by the bars. Calculations are done for two values of acceptance ($q = 1/5$, and $q = 1/9$). The dashed and dotted lines correspond to acceptance scaling Eq. (3), whereas the markers are calculated from Eq. (22). One finds that multiplicity fluctuations in bins with high transverse momentum and high values of rapidity are, due to energy and momentum conservation, essentially suppressed with respect to bins where individual particles carry less energy and momentum.

A intuitive explanation would probably look like this: Let us consider an event with an unusually large (small) number of particles at the most forward rapidity bin. In this bin we would find therefore a macroscopic state with unusually large (small) observed longitudinal momentum $P_z^{\rm obs}$ and energy $E^{\rm obs}$. The remainder of the system therefore has to have rather large (small) momentum $-P_z^{\rm obs}$ and rather small (large) energy E-$E^{\rm obs}$. Because both probability distributions, for the observed and the unobserved subsystems, do not factorize into independent probability distributions but are correlated, this macro state would be rather unlikely. Fluctuations about the mean $\langle N_y \rangle$ at forward (backward) rapidities should therefore be suppressed. However, modest multiplicity fluctuations in a high-p_T bin induce stronger fluctuations in the lower-p_T bins, and fluctuations about $\langle N_{p_T} \rangle$ in a low-p_T bin are enhanced. Even when detecting only a fraction of about 10% of the total system these correlations can have a sizable effect.

C. Conservation laws

It seems worthwhile to consider individual conservation laws and their impact on multiplicity fluctuations in more detail. One of the main advantages of the analytical procedure presented here is certainly that one can easily "switch on" or "switch off" a particular conservation law. For illustrative purposes we show the result of $\omega_{\Delta y}^{\rm mce}$ for MCE without longitudinal momentum conservation in Fig. 3.

In comparing Fig. 2, right, to Fig. 3 it becomes obvious that energy conservation alone cannot account for the strong suppression of multiplicity fluctuations at forward rapidities but has to be explained by combined energy and longitudinal momentum conservation.

The relevant cumulants elements, which give information about the strength of correlations between particle number and a particular conserved quantity, are $\kappa_2^{N_\Omega, Q}$, $\kappa_2^{N_\Omega, E}$, $\kappa_2^{N_\Omega, p_x}$, etc. Whenever a element is vanishing, then the corresponding conservation law has no impact on multiplicity fluctuations.

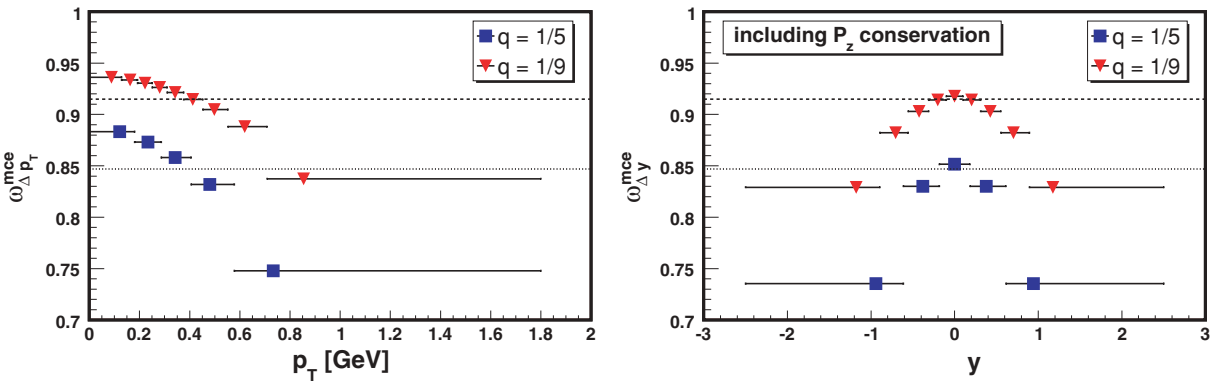

FIG. 2. (Color online) Transverse-momentum (left) and rapidity dependence (right) of the scaled variance of π^- at $T = 160$ MeV, for a classical pion gas at zero charge density. Momentum bins are constructed in a way that each bin contains the same fraction q of the average π^- yield. The (error) bars indicate the width of the p_T or y bins, whereas the marker indicate the position of the center of gravity of the corresponding bin. The lines indicate acceptance scaling Eq. (3). Calculations are done for different values of acceptance. $q = 1/5$ (square marker, dotted line), $q = 1/9$ (triangle down, dashed).

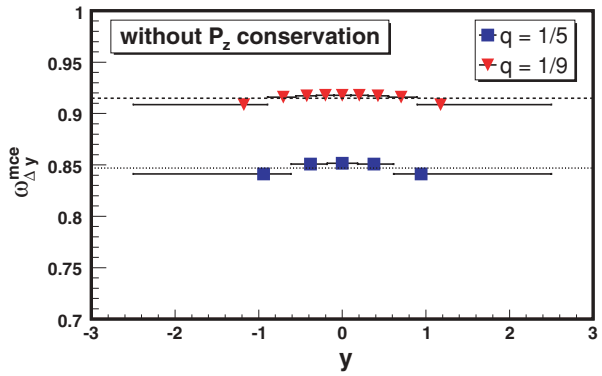

FIG. 3. (Color online) Same as Fig. 2(right) but without P_z conservation.

For details of the calculations please see the Appendix. Because for fluctuations of charged particles $\kappa_2^{N_\Omega,Q}$ and $\kappa_2^{N_\Omega,E}$ are generally nonzero, we will focus only on the effects of momentum conservation.

For multiplicity fluctuations in bins in transverse momentum, momentum conservation does not affect the result, see Appendix B, and the suppression effect is a result of energy conservation alone. When considering cuts in rapidity one finds in general $\kappa_2^{N_y,p_z} \neq 0$, but $\kappa_2^{N_y,p_x} = \kappa_2^{N_y,p_y} = 0$, and only longitudinal momentum conservation needs to be taken into account, see Appendix C. In considering the third idealized case, where our detector observes only a segment in azimuthal angle ϕ, but all rapidities y and transverse momenta p_T, both global P_x, and P_y conservation lead to nontrivial modifications of Eq. (3), see Appendix D.

To understand the difference between the strong suppression of fluctuations at high transverse momentum and the rather modest suppression at high rapidity when momentum conservation is not enforced, one should compare the elements $\kappa_2^{N_{pT},E}$ in Eq. (B3), and $\kappa_2^{N_y,E}$ in Eq. (C4), which measure in Boltzmann approximation the average energy density carried by particles in a bin Δp_T or Δy, to the total average energy density $\langle E_- \rangle = \kappa_2^{N_{4\pi},E}$ carried by π^-. [All other elements in Eqs. (B3) and (C4) do not depend on the location of the segment.] In case of kinematical cuts in Δp_T the fraction $\kappa_2^{N_{pT},E}/\langle E_- \rangle$ rises from about 5% in the lowest to roughly 20% in the highest p_T bin. In contrast to that for the central y-bin this ratio is about 10%, whereas the most forward or backward bins it is roughly 12%. However, in both cases the bins contain on average $q = 1/9 \approx 11\%$ of the total average π^- yield. The effect of energy conservation is thus weaker for cuts in rapidity than for cut in transverse momentum, see also Appendices B and C.

D. Charged systems

In Fig. 4 the transverse-momentum (left) and rapidity (right) dependence of the scaled variance is presented for two different values of charge density. Similar to the CE, in MCE the effective size of the heat and charge bath matters. We find that in general MCE effects for negatively charged particles are stronger (weaker) when the electric charge density is negative (positive). In the limit of a strongly positively charged system, the π^- subsystem could be considered as embedded in a large heat, charge, and momentum bath (provided by π^+ and π^0 particles) and MCE effects would cease. The GCE would here be the appropriate limit. In the opposite limit of a strongly negatively charged system, charge conservation essentially becomes equivalent to particle number conservation. This scenario might be more familiar from textbooks, where the CE is usually understood as the ensemble with fixed particle number. However here also the same arguments as above apply, except the effect would be much stronger, and $\omega_{4\pi}^{\rm mce} = 0$.

In general one would expect that suppression effects in bins of high transverse momentum or high values of rapidity are stronger the more abundant the analyzed particle species is. In the context of heavy-ion collision this implies that MCE effects should be stronger for positively charged particles than for negatively charged particles, due to the fact that the created system carries positive net charge.

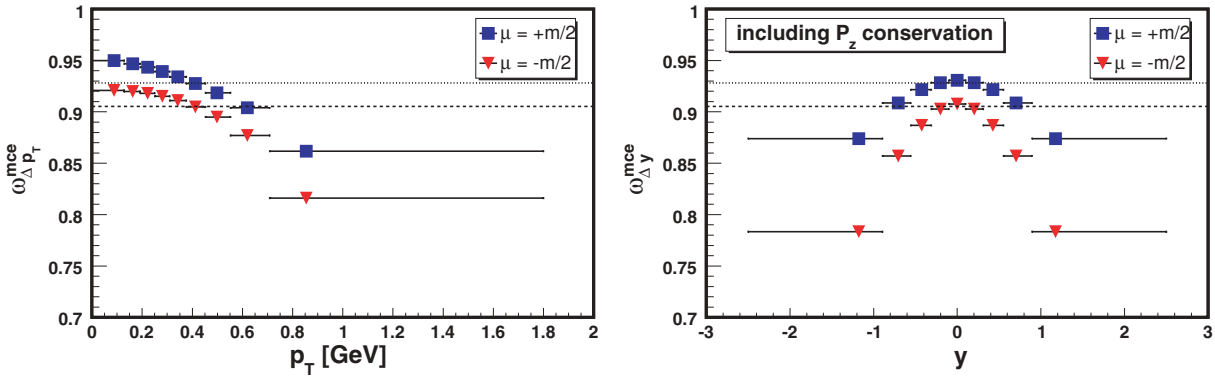

FIG. 4. (Color online) Transverse-momentum (left) and rapidity dependence (right) of the scaled variance of π^- at $T = 160$ MeV, for a classical pion gas at zero charge density. Momentum bins are constructed in a way that each bin contains the same fraction q of the average π^- yield. The (error) bars indicate the width of the p_T or y bins, whereas the markers indicate the position of the center of gravity of the corresponding bin. The lines indicate acceptance scaling Eq. (3). Calculations are done for different charge densities $\mu = -\frac{m}{2}$ (square marker, dotted) and $\mu = +\frac{m}{2}$ (triangle down, dashed).

Previous work suggests that the asymptotic values for the scaled variance are indeed reached rather quickly [15] and the above results are certainly applicable to large systems expected to be created in relativistic heavy-ion collisions.

VI. REMARKS AND CONCLUSION

Some concluding remarks seems to be in order. Although it might seem inappropriate to use the MCE formulation of a hadron resonance gas model for calculation of multiplicity fluctuations in heavy-ion collisions, as energy and volume cannot be assumed to be the same in all events, it should be stressed that GCE and CE still imply a very particular type of heat (and momentum) bath, namely an infinite (and ideal) one. This assumption seems to us even less appropriate. Also the MCE is often understood as the ensemble with energy (and charge); however, not momentum conservation. It is usually assumed that taking momentum conservation into account will not affect fluctuations in the large volume limit. We have shown [17] in a recent article that this is indeed the case, when one assumes information about all produced particles. However, for calculations of multiplicity fluctuations in arbitrary finite subsystems in momentum space all kinematic conservation laws need to be taken into account.

In a realistic heavy-ion experiment it seems impossible to measure the entire final state of each collision. The observed subsystem could therefore be seen as effectively embedded into a (possibly much larger) heat, charge, and momentum bath. Sometimes it is therefore argued that, when investigating only a small part of a statistical system (canonical or micro-canonical), one can ignore correlations of the subsystem under investigation with the remaining system. This argument is often applied when considering yields and/or fluctuations in a limited segment of momentum space. More precisely, usually the GCE is thought to be the appropriate ensemble to model fluctuations of particle multiplicity or particle ratios found in some mid-rapidity interval [28]. In this work we have argued that this assumption should be checked carefully. The GCE is the correct ensemble to choose only if heat and charge bath are assumed to be infinite, while the observed subsystem remains finite.

Based on our previous line of arguments, one would also expect that strong collective longitudinal and transverse flow would lead to a strong correlation of macroscopic subsystems. Longitudinal momentum conservation implies that when "observing" in an event a final state with a certain small (large) number of produced particles at very forward rapidity, a similarly small (large) number of particles should exist at backward rapidities. Particles in these bins carry substantial longitudinal momenta and hence energy. Modest fluctuations in their numbers should therefore induce stronger fluctuations in the central rapidity region. The same line of arguments is applicable to the transverse-momentum dependence. One would therefore expect a similar momentum space dependence of experimentally measured charged particle multiplicity fluctuations as shown in Fig. 2.

This argument is additionally supported by ultrarelativistic quantum molecular dynamics (UrQMD) model simulations [29]. In transport calculations the produced systems stay far away from global or local equilibrium [30] and other (dynamical) mechanisms might lead to similar effects. However, one could also infer from Ref. [29] that even in nonequilibrium systems correlations due to exactly enforced conservation laws determine the general trend, although transport simulations show, for instance, a very different dependence of multiplicity fluctuations on beam energy [31,32] than statistical equilibrium models. This should be subject of further investigation.

Finally, and most importantly, we want to stress that recently presented preliminary NA49 analysis of multiplicity fluctuations in certain rapidity and transverse-momentum windows [33] shows qualitatively the very same trends as they are suggested by the MCE formulation of the statistical model. Data, UrQMD simulations, and the statistical model exhibit suppressed multiplicity fluctuations when bins with high transverse momentum (or high values of rapidity) are compared to bins of same mean multiplicity at lower transverse momentum (or lower values of rapidity). We are certainly tempted to interpret this rather unexpected common behavior as a manifestation of energy and momentum conservation effects.

For a direct comparison of model calculations to experimental data [33] the formalism presented here should be essentially extended. Inclusion of the effects of resonance decay and collective motion should therefore be subject of future studies.

The cumulants defined by Eq. (18) cannot directly be related to experimentally measurable quantities. However measurement of correlation functions between "global" observables in present or future heavy-ion collision experiments, e.g., measurement of correlations between mean transverse-momentum p_T and average particle number $\langle N \rangle$ (see also Ref. [34]), fluctuations of transverse momentum [35], or any other fluctuation or correlation measure that can be related to moments of corresponding distributions, can also be related to a covariance matrix of the type shown in Eq. (27). Experimental determination of such a covariance matrix would provide valuable information on statistical properties of systems created in high-energy heavy-ion collisions. Theoretical calculation within the afore mentioned extensions to the model should therefore also be subject of future studies.

VII. SUMMARY

We have discussed the effect of momentum space cuts on multiplicity fluctuations in the framework of an ideal classical pion gas in the three standard ensembles, GCE, CE, and MCE. Only in the MCE we expect a momentum space dependence of multiplicity fluctuations when comparing intervals of same average multiplicity. We have shown that even in the thermodynamic limit energy-momentum conservation can leave a sizable effect in the fluctuation pattern.

In a previous publication we have argued that despite the fact one may expect event-by-event fluctuations of the thermal energy, i.e., the part of the total energy which goes into thermal particle production rather than collective expansion, these event-by-event fluctuations remain small compared to

energy fluctuations one would expect from grand canonical and canonical ensembles. In this work we have shown that energy and momentum conservation lead to a nontrivial momentum space dependence of the fluctuation pattern. This argument seems to be strongly supported by data.

Above results become all the more interesting when compared to models that seek to describe effects beyond our considerations. In fact our calculations suggest a similar strength of respective suppression or enhancement as they were predicted as signals for the critical point of strongly interacting matter, the onset of deconfinement, or generally a possible phase transition. One might also be tempted to argue that enhanced fluctuations around mid-rapidity, when compared to a more forward rapidity slice, should be interpreted as a signal of a phase transition from a quark gluon plasma to a hadron gas phase, expected to be first realized in the presumably hotter and denser central rapidity region. However, in this case there should be a nonmonotonic variation as center-of-mass energy of colliding nuclei is changed. This seems not to be supported by preliminary NA49 data.

In summary, the above results should be treated as a prediction for general trends of multiplicity fluctuations in limited segments of momentum space. The existence of this general behavior should be further tested by current experiments. Observation of effects similar to those of Fig. 2 in experimental data would, in our opinion, strongly speak in favor of our hypothesis that fluctuations of extensive observables are indeed dominated by material and motional conservation laws.

ACKNOWLEDGMENTS

We thank F. Becattini, V. V. Begun, M. Bleicher, E. L. Bratkovskaya, W. Broniowski, L. Ferroni, M. I. Gorenstein, M. Gaździcki, S. Häussler, V. P. Konchakovski, B. Lungwitz, and G. Torrieri for fruitful discussions.

APPENDIX A: GLOBALLY CONSERVED QUANTITIES

Turning now to calculations of cumulants, Eq. (18), we employ always coordinates most suitable to our problem. The invariant phase-space element is given by:

$$\varepsilon\frac{dN}{d^3p} = \frac{dN}{m_T\,dm_T\,dy\,d\phi} = \frac{dN}{p_T\,dp_T\,dy\,d\phi} = \varepsilon\frac{g}{(2\pi)^3}\exp\left(-\frac{\varepsilon-\mu}{T}\right), \tag{A1}$$

where the single-particle energy $\varepsilon = m_T\cosh y$, its longitudinal momentum $p_z = m_T\sinh y$, transverse mass $m_T^2 = p_T^2 + m^2$, transverse momentum $p_T^2 = p_x^2 + p_y^2$, and rapidity $y = \tanh(p_z/\varepsilon)$. Additionally we employ spherical coordinates:

$$\frac{dN}{d^3p} = \sin\theta\; p^2\frac{dN}{d\phi d\theta dp}. \tag{A2}$$

For clarity we consider explicitly a few terms, not given in Ref. [17], here. The total energy density is given by the sum over individual contributions of all particle species k:

$$\begin{aligned}\kappa_1^E &= \left(-i\frac{\partial}{\partial\phi_E}\right)\Psi(\phi_j)\Big|_{\phi_j=\vec{0}}\\ &= \sum_k\int_0^{+\pi}d\theta\int_{-\pi}^{+\pi}d\phi\int_0^{\infty}dp\varepsilon_k\frac{dN_k}{d\phi\,d\theta\,dp}\\ &= \sum_k\frac{g_k\,e^{\frac{q_k\mu}{T}}}{2\pi^2}m_k^3\,T\left[K_1\left(\frac{m_k}{T}\right)+3\frac{T}{m_k}K_2\left(\frac{m_k}{T}\right)\right]\\ &= \sum_k\langle E_k\rangle.\end{aligned} \tag{A3}$$

The diagonal energy element $\kappa_2^{E,E}$ is given by:

$$\begin{aligned}\kappa_2^{E,E} &= \left(-i\frac{\partial}{\partial\phi_E}\right)^2\Psi(\phi_j)\Big|_{\phi_j=\vec{0}}\\ &= \sum_k\int_0^{+\pi}d\theta\int_{-\pi}^{+\pi}d\phi\int_0^{\infty}dp\varepsilon_k^2\frac{dN_k}{d\phi\,d\theta\,dp}\\ &= \sum_k\frac{g_k\,e^{\frac{q_k\mu}{T}}}{2\pi^2}m_k^4\,T\left[K_0\left(\frac{m_k}{T}\right)+5\frac{T}{m_k}K_1\left(\frac{m_k}{T}\right)\right.\\ &\quad\left.+12\frac{T^2}{m_k^2}K_2\left(\frac{m_k}{T}\right)\right].\end{aligned} \tag{A4}$$

Additionally we define the diagonal momentum correlation terms, with $p_z = p\cos\theta$:

$$\begin{aligned}\kappa_2^{p_z,p_z} &= \left(-i\frac{\partial}{\partial\phi_{p_z}}\right)^2\Psi(\phi_j)\Big|_{\phi_j=\vec{0}}\\ &= \sum_k\int_0^{2\pi}d\phi\int_0^{\pi}d\theta\int_0^{\infty}dp\;p_z^2\frac{dN_k}{d\phi\,d\theta\,dp}\\ &= \sum_k\frac{g_k\,e^{\frac{q_k\mu}{T}}}{2\pi^2}m_k^4\,T\left[\frac{T}{m_k}K_1\left(\frac{m_k}{T}\right)+4\frac{T^2}{m_k^2}K_2\left(\frac{m_k}{T}\right)\right].\end{aligned} \tag{A5}$$

Due to spherical symmetry in momentum space we find $\kappa_2^{p_x,p_x} = \kappa_2^{p_y,p_y} = \kappa_2^{p_z,p_z}$. Correlation terms of odd order in one of the momenta are identical to zero. As an example we find for correlations between energy and longitudinal momentum:

$$\begin{aligned}\kappa_2^{E,p_z} &= \left(-i\frac{\partial}{\partial\phi_E}\right)\left(-i\frac{\partial}{\partial\phi_{p_z}}\right)\Psi(\phi_j)\Big|_{\phi_j=\vec{0}}\\ &= \sum_k\int_0^{2\pi}d\phi\int_0^{\pi}d\theta\int_0^{\infty}dp\varepsilon p_z\frac{dN_k}{d\phi d\theta dp} = 0,\end{aligned} \tag{A6}$$

because the integral over the polar angle $\int_0^{\pi}\sin\theta\cos\theta = 0$. Similarly we find $\kappa_2^{Q,p_x} = \kappa_2^{p_x,p_y} = 0$. Additionally $\kappa_1^{p_x} = 0$, etc., because for a static source $\langle\vec{P}\rangle = \vec{0}$.

APPENDIX B: TRANSVERSE MOMENTUM SEGMENT

The average particle number density of π^- in a segment of transverse momentum Δp_T is given by Eq. (18), i.e., the

first derivative of the CGF with respect to $\phi_{N_\Omega} = \phi_{N_{p_T}}$ at the origin:

$$\begin{aligned}\kappa_1^{N_{p_T}} &= \left(-i\frac{\partial}{\partial\phi_{N_{p_T}}}\right)\Psi(\phi_j)\Big|_{\phi_j=\vec{0}} \\ &= \int_{\Delta p_T} dp_T \int_0^{2\pi} d\phi \int_{-\infty}^{\infty} dy \frac{dN}{dp_T\, dy\, d\phi} \\ &= \frac{g e^{-\frac{\mu}{T}}}{2\pi^2}\int_{\Delta p_T} dp_T\, p_T \sqrt{p_T^2+m^2} K_1\left(\frac{\sqrt{p_T^2+m^2}}{T}\right).\end{aligned} \tag{B1}$$

Please note that $\kappa_1^{N_{p_T}} = \int_{\Delta p_T} dp_T dN/dp_T = \langle N_{p_T}\rangle$. Correlations of π^- in a segment Δp_T with globally conserved energy are given by double differentiation of $\Psi(\phi_j)$ with respect to $\phi_{N_{p_T}}$ and ϕ_E, thus:

$$\begin{aligned}\kappa_2^{N_{p_T},E} &= \left(-i\frac{\partial}{\partial\phi_{N_{p_T}}}\right)\left(-i\frac{\partial}{\partial\phi_E}\right)\Psi(\phi_j)\Big|_{\phi_j=\vec{0}} \\ &= \int_{\Delta p_T} dp_T \int_0^{2\pi} d\phi \int_{-\infty}^{\infty} dy\varepsilon \frac{dN}{dp_T\, dy\, d\phi} \\ &= \frac{g e^{-\frac{\mu}{T}}}{2\pi^2}\int_{\Delta p_T} dp_T\, p_T\left(p_T^2+m^2\right)\left[K_0\left(\frac{\sqrt{p_T^2+m^2}}{T}\right)\right. \\ &\quad \left. + \frac{T}{\sqrt{p_T^2+m^2}} K_1\left(\frac{\sqrt{p_T^2+m^2}}{T}\right)\right].\end{aligned} \tag{B2}$$

Correlations between conserved momenta and particles in Δp_T, given by the elements $\kappa_2^{N_{p_T},p_x}$, $\kappa_2^{N_{p_T},p_y}$, and $\kappa_2^{N_{p_T},p_z}$ are identical to zero, due to symmetry in azimuthal angle ϕ for the first two and due to an antisymmetric rapidity integral for the last. Therefore, all elements involving an odd order in one of the momenta in Eq. (27) are equal to zero. The determinant of Eq. (27) thus factorizes, similarly to Eq. (26), into a product of $(\kappa_2^{p_x,p_x})^3$ and the determinant of a 3×3 submatrix involving only terms containing N_{p_T}, E, Q. Hence momentum conservation drops out when calculating Eq. (22). However, the strength of correlations between particle number N_{p_T} and globally conserved energy E will depend on the position of the segment Δp_T. Thus using Eqs. (22) and (27), one can express the width of the MCE multiplicity distribution (21) by:

$$\begin{aligned}\omega_{\Delta p_T}^{mce} &= \frac{\kappa_2^{N_{p_T},N_{p_T}}}{\kappa_1^{N_{p_T}}} - \frac{1}{\kappa_1^{N_{p_T}}\det|\hat{\kappa}_2|}\left[\left(\kappa_2^{N_{p_T},Q}\right)^2\kappa_2^{E,E}\right. \\ &\quad \left. + \left(\kappa_2^{N_{p_T},E}\right)^2\kappa_2^{Q,Q} - 2\kappa_2^{N_{p_T},E}\kappa_2^{N_{p_T},Q}\kappa_2^{E,Q}\right]\end{aligned} \tag{B3}$$

In Boltzmann approximation, we find from Eq. (18), $\kappa_2^{N_{p_T},N_{p_T}} = \kappa_2^{N_{p_T},Q} = \kappa_1^{N_{p_T}} = q\kappa_1^{N_{4\pi}}$, where we have defined the acceptance $q \equiv \kappa_1^{N_{p_T}}/\kappa_1^{N_{4\pi}}$. However, when observing a fraction q of the particle density, one does not necessarily observe the same fraction q of the energy density $\langle E_-\rangle$ carried by π^-, and thus $\kappa_2^{N_{p_T},E} \neq q\langle E_-\rangle$. Therefore depending on the location of Δp_T, our detector sees a larger (smaller) fraction of the total energy, which leads to smaller (larger) particle number fluctuations, see Fig. 2(left). One can easily verify that setting $\kappa_2^{N_{p_T},E} = q\langle E_-\rangle$ in Eq. (B3), leads to acceptance scaling, Eq. (3), $\omega_{\Delta p_T}^{\rm mce} = 1 + q(\omega_{4\pi}^{\rm mce} - 1)$.

APPENDIX C: RAPIDITY SEGMENT

The average particle number density of π^- in a rapidity interval Δy is given by:

$$\begin{aligned}\kappa_1^{N_y} &= \left(-i\frac{\partial}{\partial\phi_{N_y}}\right)\Psi(\phi_j)\Big|_{\phi_j=\vec{0}} \\ &= \int_m^{\infty} dm_T \int_0^{2\pi} d\phi \int_{\Delta y} dy \frac{dN}{dm_T\, dy\, d\phi} \\ &= \frac{g e^{-\frac{\mu}{T}}}{(2\pi)^2} T^3 \int_{\Delta y} dy \exp\left[-\frac{m}{T}\cosh(y)\right] \\ &\quad \times \left[\left(\frac{m}{T}\right)^2 + 2\frac{m}{T}\cosh^{-1} y + 2\cosh^{-2} y\right].\end{aligned} \tag{C1}$$

Please note that $\kappa_1^{N_y} = \int_{\Delta y} dy dN/dy = \langle N_y\rangle$. Correlations of particles in Δy with globally conserved energy are given by:

$$\begin{aligned}\kappa_2^{N_y,E} &= \left(-i\frac{\partial}{\partial\phi_{N_y}}\right)\left(-i\frac{\partial}{\partial\phi_E}\right)\Psi(\phi_j)\Big|_{\phi_j=\vec{0}} \\ &= \int_m^{\infty} dm_T \int_0^{2\pi} d\phi \int_{\Delta y} dy\varepsilon \frac{dN}{dm_T\, dy\, d\phi} \\ &= \frac{g e^{-\frac{\mu}{T}}}{(2\pi)^2} T^4 \int_{\Delta y} dy \cosh y \exp\left(-\frac{m}{T}\cosh y\right)\left[\left(\frac{m}{T}\right)^3\right. \\ &\quad \left. + 3\left(\frac{m}{T}\right)^2\cosh^{-1} y + 6\frac{m}{T}\cosh^{-2} y + 6\cosh^{-3} y\right].\end{aligned} \tag{C2}$$

The correlation term of particles in Δy with globally conserved longitudinal momentum P_z reads:

$$\begin{aligned}\kappa_2^{N_y,p_z} &= \left(-i\frac{\partial}{\partial\phi_{N_y}}\right)\left(-i\frac{\partial}{\partial\phi_{p_z}}\right)\Psi(\phi_j)\Big|_{\phi_j=\vec{0}} \\ &= \int_0^{2\pi} d\phi \int_m^{\infty} dm_T \int_{\Delta y} dy p_z \frac{dN}{dm_T\, dy\, d\phi} \\ &= \frac{g e^{-\frac{\mu}{T}}}{(2\pi)^2} T^4 \int_{\Delta y} dy \sinh y \exp\left(-\frac{m}{T}\cosh y\right)\left[\left(\frac{m}{T}\right)^3\right. \\ &\quad \left. + 3\left(\frac{m}{T}\right)^2\cosh^{-1} y + 6\frac{m}{T}\cosh^{-2} y + 6\cosh^{-3} y\right].\end{aligned} \tag{C3}$$

Thus the element $\kappa_2^{N_y,p_z}$ in the matrix (27) is nonvanishing, and longitudinal momentum (P_z) conservation seems to affects correlations between particles in a segment Δy and the remaining system. In contrast to that further elements are equal to zero, $\kappa_2^{N_y,p_x} = \kappa_2^{N_y,p_y} = 0$, and P_x and P_y conservation have no additional effect. When momentum conservation is taken into account the scaled variance (22) can be calculated from Eq. (25):

$$\omega_{\Delta y}^{\mathrm{mce}} = \frac{\kappa_2^{N_y,N_y}}{\kappa_1^{N_y}} - \frac{1}{\kappa_1^{N_y}\kappa_2^{p_z,p_z}\det|\hat{\kappa}_2|}\Big\{\big(\kappa_2^{N_y,Q}\big)^2\kappa_2^{E,E}\kappa_2^{p_z,p_z} + \big(\kappa_2^{N_y,E}\big)^2\kappa_2^{Q,Q}\kappa_2^{p_z,p_z} + \big(\kappa_2^{N_y,p_z}\big)^2\big[\kappa_2^{Q,Q}\kappa_2^{E,E} - \big(\kappa_2^{E,Q}\big)^2\big] - 2\kappa_2^{p_z,p_z}\kappa_2^{N_y,E}\kappa_2^{N_y,Q}\kappa_2^{E,Q}\Big\}. \quad \text{(C4)}$$

Similarly to the previous section, we find a large (small) $\kappa_2^{N_y,p_z}$ leads to small (large) fluctuations, see Fig. 2(right). When intervals symmetric in rapidity are assumed, e.g., $\Delta y = [-y_1, y_1]$, or $\Delta y = [-y_2, -y_1] \cup [y_1, y_2]$, correlations between particle number and momentum disappear, $\kappa_2^{N_y,p_z} = 0$, and Eq. (C4) reduces to Eq. (B3), and momentum conservation does not play a role. Equally when disregarding longitudinal momentum conservation the same arguments as those of Appendix B apply and Eq. (B3) holds; however, the effect is much weaker, see Fig. 3.

APPENDIX D: AZIMUTHAL ANGLE SEGMENT

Th average particle number in $\Delta\phi$, whereas integrating over all p_T and y is simply a fraction $q = \Delta\phi/2\pi$ of the total yield $\langle N_{4\pi}\rangle$. Therefore $\kappa_1^{N_\phi} = q\kappa_1^{N_{4\pi}}$. Equally, the energy carried by π^- in this interval is $\kappa_2^{E,N_\phi} = q\langle E_-\rangle$. Due to symmetry around $y = 0$, we find additionally $\kappa_2^{N_\phi,p_z} = 0$. However, for the transverse momenta $p_x = p_T\cos\phi$, and $p_y = p_T\sin\phi$ the correlation with N_ϕ is generally nonzero.

$$\begin{aligned}\kappa_2^{N_\phi,p_x} &= \left(-i\frac{\partial}{\partial\phi_{N_\phi}}\right)\left(-i\frac{\partial}{\partial\phi_{p_x}}\right)\Psi(\phi_j)\Big|_{\phi_j=\vec{0}} \\ &= \frac{g}{(2\pi)^3}\int_{\Delta\phi}d\phi\int_0^\infty dp_T\int_{-\infty}^\infty dy p_x\frac{dN}{dp_T\,dy\,d\phi} \\ &= \int_{\Delta\phi}d\phi\cos\phi\frac{2ge^{-\frac{\mu}{T}}}{(2\pi)^3}m^2T\sqrt{\frac{\pi}{2}mT}K_{5/2}\left(\frac{m}{T}\right) \\ &= (2\pi)^{-1}(\sin\phi)_{\Delta\phi}\langle p_T\rangle. \end{aligned} \quad \text{(D1)}$$

Similarly we find $\kappa_2^{N_\phi,p_y} = -(2\pi)^{-1}[\cos\phi]_{\Delta\phi}\langle p_T\rangle$. Unlike in the previous sections there is no particular dependence of the position of the interval $\Delta\phi$. However, in general there is a dependence. When momentum conservation is taken into account Eq. (22) can be calculated from Eq. (25):

$$\omega_{\Delta\phi}^{mce} = \frac{\kappa_2^{N_\phi,N_\phi}}{\kappa_1^{N_\phi}} - \frac{1}{\kappa_1^{N_\phi}\kappa_2^{p_x,p_x}\det|\hat{\kappa}_2|}\Big\{\big(\kappa_2^{N_\phi,Q}\big)^2\kappa_2^{E,E}\kappa_2^{p_x,p_x} + \big(\kappa_2^{N_\phi,E}\big)^2\kappa_2^{Q,Q}\kappa_2^{p_x,p_x} + \Big[\big(\kappa_2^{N_\phi,p_x}\big)^2 + \big(\kappa_2^{N_\phi,p_y}\big)^2\Big] \times\big[\kappa_2^{Q,Q}\kappa_2^{E,E} - \big(\kappa_2^{E,Q}\big)^2\big] - 2\kappa_2^{p_x,p_x}\kappa_2^{N_\phi,E}\kappa_2^{N_\phi,Q}\kappa_2^{E,Q}\Big\}, \quad \text{(D2)}$$

where we have used $\kappa_2^{p_x,p_x} = \kappa_2^{p_y,p_y}$. As mentioned before there is no particular dependence of $\kappa_2^{N_\phi,E}$ and $\kappa_2^{N_\phi,Q}$ on the position of $\Delta\phi$. However we have a term $(\kappa_2^{N_\phi,p_x})^2 + (\kappa_2^{N_\phi,p_y})^2$. In case we assume a continuous interval $\Delta\phi_A = [\phi_1, \phi_2]$ this terms reads:

$$\big(\kappa_2^{N_\phi,p_x}\big)^2 + \big(\kappa_2^{N_\phi,p_y}\big)^2 = \frac{\langle p_T\rangle^2}{(2\pi)^2}[1 - \cos(\phi_1 - \phi_2)]. \quad \text{(D3)}$$

This term is evidently positive, hence fluctuations are suppressed. One can easily verify that when one takes $\Delta\phi_B = [\phi_1, \phi_2] \cup [\phi_1 + \pi, \phi_2 + \pi]$, i.e., two opposite slices in azimuthal angle, the correlation disappears, $\kappa_2^{N_\phi,p_x} = \kappa_2^{N_\phi,p_y} = 0$, and one returns to acceptance scaling, Eq. (3).

[1] J. Cleymans, H. Oeschler, K. Redlich, and S. Wheaton, Phys. Rev. C **73**, 034905 (2006).
[2] F. Becattini, J. Manninen, and M. Gaździcki, Phys. Rev. C **73**, 044905 (2006).
[3] A. Andronic, P. Braun-Munzinger, and J. Stachel, Nucl. Phys. **A772**, 167 (2006).
[4] J. Letessier and J. Rafelski, arXiv:nucl-th/0504028.
[5] B. Lungwitz *et al.* (NA49 Collaboration), PoS C **FRNC2006**, 024 (2006).
[6] V. V. Begun, M. Gaździcki, M. I. Gorenstein, M. Hauer, V. P. Konchakovski, and B. Lungwitz, Phys. Rev. C **76**, 024902 (2007).
[7] V. V. Begun, M. Gaździcki, M. I. Gorenstein, and O. S. Zozulya, Phys. Rev. C **70**, 034901 (2004).
[8] H. Heiselberg, Phys. Rep. **351**, 161 (2001); S. Jeon and V. Koch, in *Quark-Gluon Plasma* 3, edited by R. C. Hwa and X.-N. Wang (World Scientific, Singapore, 2004), p. 430.
[9] M. Gaździcki, M. I. Gorenstein, and S. Mrowczynski, Phys. Lett. **B585**, 115 (2004); M. I. Gorenstein, M. Gaździcki, and O. S. Zozulya, Phys. Lett. **B585**, 237 (2004).
[10] I. N. Mishustin, Phys. Rev. Lett. **82**, 4779 (1999); H. Heiselberg and A. D. Jackson, Phys. Rev. C **63**, 064904 (2001).
[11] M. A. Stephanov, K. Rajagopal, and E. V. Shuryak, Phys. Rev. Lett. **81**, 4816 (1998); Phys. Rev. D **60**, 114028 (1999); M. Stephanov, Acta Phys. Pol. B **35**, 2939 (2004).
[12] S. Häussler, S. Scherer, and M. Bleicher, Phys. Lett. **B660**, 197 (2008).
[13] T. K. Nayak, Int. J. Mod. Phys. E **16**, 3303 (2008).
[14] V. V. Begun, M. I. Gorenstein, M. Hauer, V. P. Konchakovski, and O. S. Zozulya, Phys. Rev. C **74**, 044903 (2006).
[15] F. Becattini, A. Keränen, L. Ferroni, and T. Gabbriellini, Phys. Rev. C **72**, 064904 (2005).
[16] M. I. Gorenstein, M. Hauer, and D. O. Nikolajenko, Phys. Rev. C **76**, 024901 (2007).

[17] M. Hauer, V. V. Begun, and M. I. Gorenstein, arXiv:0706.3290 [nucl-th].
[18] V. V. Begun and M. I. Gorenstein, Phys. Rev. C **73**, 054904 (2006); V. V. Begun, M. I. Gorenstein, A. P. Kostyuk, and O. S. Zozulya, J. Phys. G **32**, 935 (2006).
[19] K. Redlich and L. Turko, Z. Phys. C **5**, 201 (1980); L. Turko, Phys. Lett. **B104**, 153 (1981); R. Hagedorn and K. Redlich, Z. Phys. C **27**, 541 (1985).
[20] J. Cleymans, K. Redlich, and E. Suhonen, Z. Phys. C **51**, 137 (1991); A. Keränen and F. Becattini, Phys. Rev. C **65**, 044901 (2002); F. Becattini and U. W. Heinz, Z. Phys. C **76**, 269 (1997).
[21] O. Fochler, S. Vogel, M. Bleicher, C. Greiner, P. Koch-Steinheimer, and Z. Xu, Phys. Rev. C **74**, 034902 (2006).
[22] C. M. Ko, V. Koch, Z. W. Lin, K. Redlich, M. A. Stephanov, and X. N. Wang, Phys. Rev. Lett. **86**, 5438 (2001).
[23] S. Jeon, V. Koch, K. Redlich, and X. N. Wang, Nucl. Phys. **A697**, 546 (2002).
[24] F. Becattini and L. Ferroni, Eur. Phys. J. C **35**, 243 (2004); **38**, 225 (2004).
[25] J. Letessier, A. Tounsi, and J. Rafelski, Phys. Lett. **B475**, 213 (2000); J. Rafelski and J. Letessier, Phys. Rev. Lett. **85**, 4695 (2000).
[26] P. Koch, B. Muller, and J. Rafelski, Phys. Rep. **142**, 167 (1986).
[27] V. V. Begun, M. I. Gorenstein, and O. S. Zozulya, Phys. Rev. C **72**, 014902 (2005).
[28] S. Jeon and V. Koch, Phys. Rev. Lett. **83**, 5435 (1999); G. Torrieri, S. Jeon, and J. Rafelski, Phys. Rev. C **74**, 024901 (2006); G. Torrieri, Int. J. Mod. Phys. E **16**, 1783 (2007).
[29] B. Lungwitz and M. Bleicher, Phys. Rev. C **76**, 044904 (2007).
[30] E. L. Bratkovskaya, W. Cassing, C. Greiner, M. Effenberger, U. Mosel, and A. Sibirtsev, Nucl. Phys. **A681**, 84 (2001); L. V. Bravina *et al*., Phys. Rev. C **60**, 024904 (1999).
[31] V. P. Konchakovski, M. I. Gorenstein, and E. L. Bratkovskaya, Phys. Lett. **B651**, 114 (2007).
[32] V. P. Konchakovski, M. I. Gorenstein, and E. L. Bratkovskaya, Phys. Rev. C **76**, 031901 (2007).
[33] B. Lungwitz *et al*. (NA49 Collaboration), arXiv:0709.1646 [nucl-ex].
[34] S. Mrowczynski, M. Rybczynski, and Z. Wlodarczyk, Phys. Rev. C **70**, 054906 (2004).
[35] H. Appelshauser *et al*. (NA49 Collaboration), Phys. Lett. **B459**, 679 (1999); D. Adamova *et al*. (CERES Collaboration), Nucl. Phys. **A727**, 97 (2003); T. Anticic *et al*. (NA49 Collaboration), Phys. Rev. C **70**, 034902 (2004); S. S. Adler *et al*. (PHENIX Collaboration), Phys. Rev. Lett. **93**, 092301 (2004); J. Adams *et al*. (STAR Collaboration), Phys. Rev. C **71**, 064906 (2005).